Plaquette order in the SU(6) Heisenberg model on the honeycomb lattice

Nataf, P.; Lajkó, M.; Corboz, P.; Läuchli, A.M.; Penc, K.; Mila, F.

DOI
10.1103/PhysRevB.93.201113

Publication date
2016

Document Version
Final published version

Published in
Physical Review B

PHYSICAL REVIEW B **93**, 201113(R) (2016)

Plaquette order in the SU(6) Heisenberg model on the honeycomb lattice

Pierre Nataf,[1] Miklós Lajkó,[2] Philippe Corboz,[3] Andreas M. Läuchli,[4] Karlo Penc,[5,6] and Frédéric Mila[1]

[1]*Institute of Physics, Ecole Polytechnique Fédérale de Lausanne (EPFL), CH-1015 Lausanne, Switzerland*
[2]*Institute for Solid State Physics, University of Tokyo, Kashiwa 277-8581, Japan*
[3]*Institute for Theoretical Physics, University of Amsterdam, 1090 GL Amsterdam, The Netherlands*
[4]*Institut für Theoretische Physik, Universität Innsbruck, A-6020 Innsbruck, Austria*
[5]*Institute for Solid State Physics and Optics, Wigner Research Centre for Physics, Hungarian Academy of Sciences, P.O.B. 49, H-1525 Budapest, Hungary*
[6]*MTA-BME Lendület Magneto-optical Spectroscopy Research Group, H-1111 Budapest, Hungary*

(Received 2 February 2016; revised manuscript received 26 April 2016; published 26 May 2016)

We revisit the SU(6) Heisenberg model on the honeycomb lattice, which has been predicted to be a chiral spin liquid by mean-field theory [G. Szirmai *et al.*, Phys. Rev. A **84**, 011611(R) (2011)]. Using exact diagonalizations of finite clusters, infinite projected entangled pair state simulations, and variational Monte Carlo simulations based on Gutzwiller projected wave functions, we provide strong evidence that the model with one particle per site and nearest-neighbor exchange actually develops plaquette order. This is further confirmed by the investigation of the model with a ring-exchange term, which shows that there is a transition between the plaquette state and the chiral state at a finite value of the ring-exchange term.

DOI: 10.1103/PhysRevB.93.201113

With the recent progress towards achieving SU(N) symmetry with ultracold fermionic atoms [1–10], the investigation of the effective SU(N) Heisenberg model on various one-dimensional (1D) and two-dimensional (2D) lattices has become a very active field of research. Several remarkable ground state properties have been reported, including long-range color order [11], algebraic correlations [12], translational symmetry breaking valence-bond solid states in which groups of N atoms form local singlets on plaquettes [13,14], and chiral ground states, suggested by Hermele *et al.* [15,16] for Mott insulators on a square lattice with several particles per site. Interestingly, a mean-field calculation even predicted a chiral spin liquid in the SU(6) Heisenberg model on the honeycomb lattice with only one particle per site [17,18]. However, the rather natural plaquette state in which six SU(6) spins form singlets on nonadjacent hexagons was found to lie very close in energy. So this result calls for further investigation with methods that go beyond mean-field theory.

In this Rapid Communication, we have addressed this problem with state-of-the-art numerical methods: variational Monte Carlo (VMC) simulations based on Gutzwiller projected wave functions, exact diagonalizations (ED), and infinite projected entangled pair state simulations (iPEPS). VMC confirmed that the two phases are very close in energy, with the plaquette state being just slightly lower in energy. Only after turning to exact diagonalizations and iPEPS could we find compelling evidence that the ground state indeed has plaquette order. The chiral state is not far in parameter space, however, and it does not take a large ring-exchange term to stabilize it, as demonstrated by ED and VMC.

The SU(6) Heisenberg model is defined by the Hamiltonian

$$\mathcal{H} = \sum_{\langle i,j\rangle} P_{ij}, \tag{1}$$

where the operator $P_{ij} = \sum_{\alpha,\beta} |\alpha_i \beta_j\rangle\langle\beta_i \alpha_j|$ exchanges the $N = 6$ colors α and β of the atoms on neighboring sites i, j of a honeycomb lattice.

VMC. Gutzwiller projected wave functions [19,20] offer a qualitative and potentially quantitative description for both types of competing scenarios found by mean-field study [17]. In this method we project out the configurations having multiple occupancy from the Fermi-sea constructed from a mean-field model. The variational parameters are the hopping amplitudes and the artificial fluxes given by their total phase around the elementary hexagons (plaquettes). An importance sampling Monte Carlo method was used to calculate the energies and correlations of the projected states [12]. Our calculations (shown in Fig. 1) reveal that the lowest energy states are similar to those of Ref. [17]: (i) a configuration with uniform $2\pi/3$ flux before projection, corresponding to a chiral spin liquid [21], and (ii) a translation symmetry breaking configuration with 0 flux in a center plaquette surrounded by π flux plaquettes with nonuniform hopping integrals, corresponding to a plaquette-ordered phase. While the mean-field results of Ref. [17] favored the chiral phase, the plaquette-ordered phase turned out, after projection, to have a slightly lower energy (see Table I), the first hint that the system might actually have a plaquette ground state. However, the energy difference becomes very small upon increasing the size. So we have decided to attack the model with alternative methods.

ED. With the standard exact diagonalization approach that takes into account all spatial symmetries but only an Abelian subgroup of the SU(N) symmetry group (color conservation plus cyclic color permutations), the currently largest accessible cluster with a number of sites multiple of 6 (a requirement for having a singlet ground state) is an 18-site cluster. The spectrum is shown in Fig. 2(a). The plaquette state is expected to be threefold degenerate in the thermodynamic limit (one state at the Γ point and two states at the two K points in the Brillouin zone), but in the 18-site cluster the plaquettes can also wrap around the torus [14], artificially enlarging the number of plaquette coverings to 6. By contrast, the chiral state is $2 \times N = 2 \times 6 = 12$-fold degenerate in the spontaneous time-reversal symmetry (TRS) breaking scenario. While the

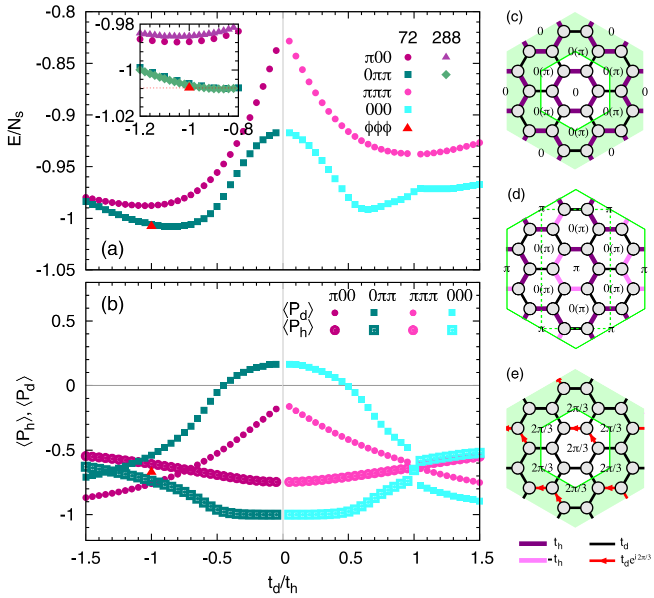

FIG. 1. (a) Energies of Gutzwiller projected wave functions and (b) the bond energies on t_d and t_h bonds after projection for the different flux configurations as a function of t_d/t_h for $N_s = 72$. (c)–(e) shows the considered flux configurations, where black bonds represent hopping amplitude t_d, while dark and light purple bonds denote hopping amplitudes t_h and $-t_h$, respectively. In the case of the uniform $2\pi/3$ flux configuration, red arrows represent complex hopping amplitude $\propto e^{i2\pi/3}$, for which $t_{ji} = t_{ij}^*$.

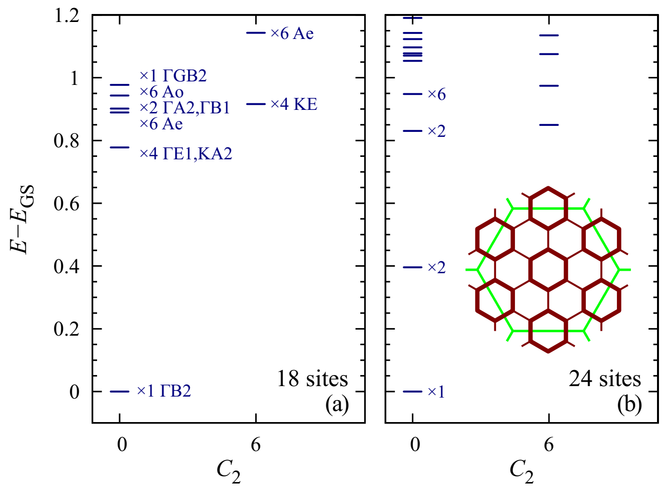

FIG. 2. Spectrum of the 18-site (left) and 24-site (right) clusters as a function of the quadratic Casimir $\mathcal{C}_2$. The degeneracies of some states are indicated, as well as the spatial quantum numbers for the 18-site cluster. For the 24-site cluster, the presence of three low-lying states is a strong indication of a plaquette phase (see text for details). Inset: Broken-symmetry plaquette state reconstructed from ED. It breaks translations, but the D_6 symmetry is preserved. The bond energy is -0.81 (-0.56) for the thick (thin) lines.

first three levels ΓB_2, $KA_2(2\times)$ (plus the symmetry related level ΓE_1 particular to $N_s = 18$) are in agreement with the expectations for a plaquette state, [14] these states are very close to many other excited states (including nonsinglets). So the spectrum does not provide enough evidence for either of the competing states.

To go further, we have used a newly developed method [22] that allows one to take advantage of the full SU(N) symmetry, hence to work directly in the irreducible representations of SU(N). For the singlet and the smallest values of the Casimir operator, this leads to Hilbert spaces of much smaller dimension than the standard approach. The spectrum is shown in Fig. 2(b). Interestingly enough, on 24 sites, the spectrum consists of three low-lying states reasonably well separated from the rest of the spectrum, the first indication that the ground state might have plaquette order. The spin-spin and dimer-dimer correlations are shown in Fig. 3. The spin-spin correlations decay quite fast, consistent with some kind of spin liquid, and the dimer-dimer correlations are consistent with a plaquette phase on the honeycomb lattice [see, for instance, the discussion of the SU(3) case in Ref. [14]].

As an additional test, we have determined the spatial quantum numbers of the first excited doublet by applying one of the two elementary translations of the lattice. The corresponding eigenstates belong to the two K points in the Brillouin zone. The correlations in these states are very similar to those in the ground state, which suggests that these three states could correspond to the degenerate ground state of the thermodynamic limit split by finite-size effects. To demonstrate that this is the case, we have constructed the symmetric sum of these states, which corresponds to the finite-size approximation of a broken-symmetry state (a simple task since the numerical wave functions are real and not complex). In that state, the strong bonds correspond to a covering of the lattice with hexagons [see the inset of Fig. 2(b)], with a difference between strong and weak bond energies of 0.25, in good agreement with the extrapolated iPEPS estimate [see Fig. 4(c) below].

However, one should not forget that we have access to only one cluster with the appropriate number of low-lying states, and that the gap to the next levels is comparable to the gap between the ground state and the first pair of low-lying states. So, below, we turn to the results obtained with iPEPS.

TABLE I. VMC energies of Gutzwiller projected wave functions for the competing $0\pi\pi$ (plaquette) and the $2\pi/3$ flux configurations for different system sizes, compared to the mean-field (MF) and iPEPS ($D = 36$) results. The statistical error of the calculations is smaller than $O(10^{-4})$. The optimized energies are obtained by considering the overlap between projected states with different boundary conditions before projection.

N_s	24	24 opt	72	72 opt	288	MF [17]	iPEPS
Plaquette	-1.039	-1.057	-1.0079	-1.0123	-1.0082	-1.010	-1.031
$\frac{2\pi}{3}$ chiral	-1.0064	-1.0104	-1.0077	-1.0087	-1.0077	-1.025	

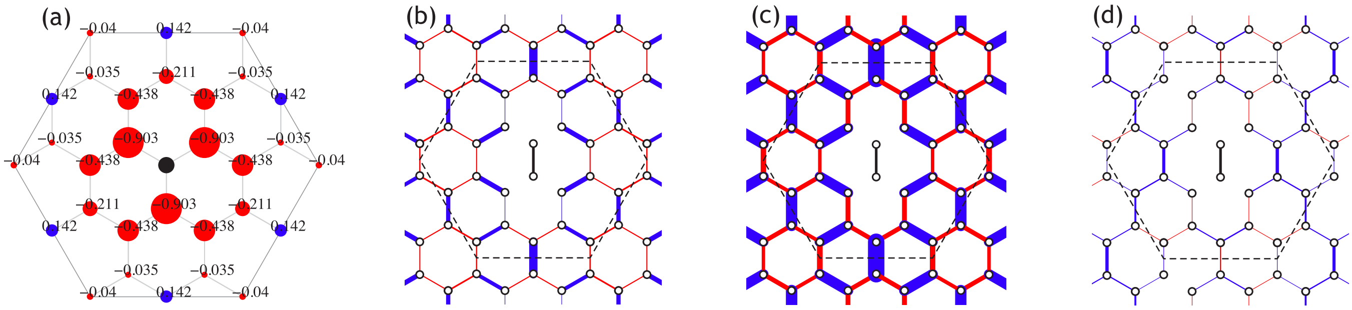

FIG. 3. (a) $\langle P_{0i}\rangle - 1/6$ spin-spin and (b) $\langle P_{12}P_{kl}\rangle - \langle P_{12}\rangle\langle P_{kl}\rangle$ dimer-dimer correlations in the exact ground state of the 24-site cluster. As a reference, we present the dimer-dimer correlations of the translational invariant linear combination of (c) the variational $0\pi\pi$ flux projected states with $|t_d/t_h| = 0.8$, and of (d) the variational $2\pi/3$ flux projected state. The pattern of the dimer-dimer correlations of (b) the ED and (c) the $0\pi\pi$ variational states is an indication of long-range plaquette ordering.

iPEPS. An iPEPS is a variational tensor network ansatz to represent a 2D wave function in the thermodynamic limit [23–25]. The ansatz on the honeycomb lattice consists of a unit cell of rank-4 tensors which is periodically repeated on the infinite lattice, for each tensor one physical index carries the local Hilbert space of lattice site, and three auxiliary indices connect to the nearest-neighbor tensors. The accuracy of the ansatz can be systematically controlled by the bond dimension D of the auxiliary indices. For the experts we note that the contraction of the tensor network is performed using a variant [26,27] of the corner-transfer matrix method [28,29], and the optimization is done by an imaginary time evolution using a combined simple and (fast) full update [30,31]. To increase the efficiency of the simulations we make use of Abelian symmetries [32,33]. A similar approach has been used in previous calculations of SU(N) Heisenberg models (see, e.g., Refs. [12,14]). For an introduction to iPEPS we refer to Refs. [30,31].

We have used a six-site unit cell which is compatible with both plaquette and uniform (possibly chiral) states. As initial states we started either from completely random tensors or from a plaquette state made of SU(6) singlets on hexagons. In the former case, using bond dimensions up to $D = 24$, a new competing state appears, in which each site in the unit cell exhibits a different dominant color. For $D \leqslant 24$ this color-ordered state has a lower variational energy than the plaquette state, as shown in Fig. 4(a). However, the slope in $1/D$ is larger for the plaquette state. So we have pushed the calculation to very large values of D, up to $D = 36$. Around $D = 30$ the energies of the two ordered states indeed cross such that the plaquette state clearly becomes energetically favored. We have not found a competing uniform chiral state with iPEPS, which is an indication that at least for the bond dimensions studied here the plaquette state is the lowest energy state.

In Fig. 4(b) we present the results for the color-order parameter of the two competing states, given by the local moment

$$m = \sqrt{\frac{6}{5}\sum_{\alpha,\beta}\left(\langle S_\alpha^\beta\rangle - \frac{\delta_{\alpha\beta}}{6}\right)^2}, \qquad (2)$$

averaged over all sites in the unit cell, where $S_\alpha^\beta = |\alpha\rangle\langle\beta|$ are the SU(6) spin operators and α,β run over all local basis states. For the color-ordered state m is large for low D. It decreases with increasing D but tends to a finite value in the infinite D limit. The local moment of the plaquette state is much more strongly suppressed with increasing D, and vanishes in the large D limit, consistent with a singlet without color order.

Figure 4(c) shows the difference between the highest and lowest bond energy in the unit cell which measures the magnitude of the plaquette order. For the color-ordered state

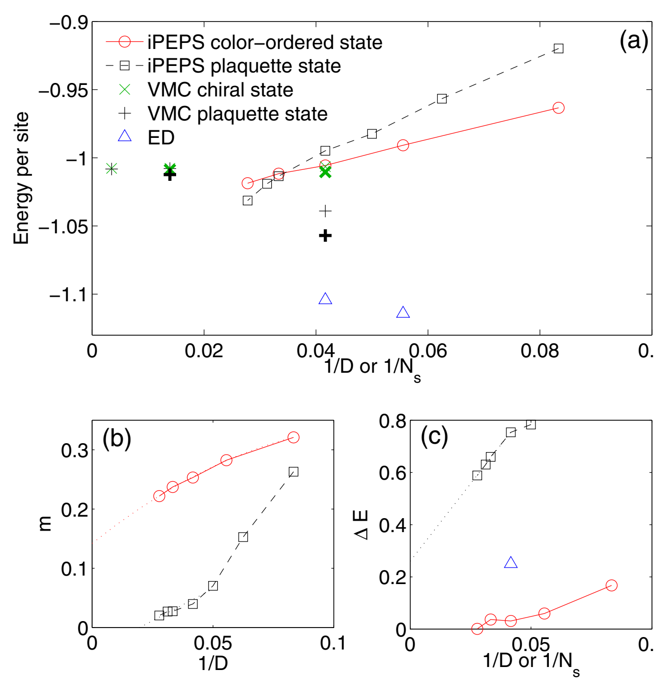

FIG. 4. iPEPS results for the SU(6) Heisenberg model on the honeycomb lattice. (a) Comparison of the ground state energy obtained with iPEPS, VMC, and ED, as a function of inverse bond dimension D and inverse system size. The bold symbols mark improved VMC results for $N_s = 24$ and 72 (see Table I and main text). For large bond dimension with iPEPS the plaquette state has the lowest variational energy, in agreement with VMC. (b) Color-order parameter as a function of inverse D. It is finite for the color-ordered state and vanishes for the plaquette state. (c) Difference in energy between the strongest bond and the weakest bond in the unit cell, which is strongly suppressed in the color-order state, and finite in the plaquette state, consistent with plaquette long-range order. The dotted lines are a guide to the eye.

it is strongly suppressed with increasing D and vanishes for large D, in contrast to the plaquette state which exhibits a large difference in bond energy, where the strong bonds form hexagonal plaquettes.

Ring-exchange term. Since the energy difference between the plaquette and chiral phases found by VMC is very small, it is tempting to speculate that the chiral phase might be stabilized by a ring-exchange term around the hexagons. We have thus considered

$$\mathcal{H} = \cos\theta \sum_{\langle i,j\rangle} P_{ij} + \sin\theta \sum_{\text{plaquettes}} i(P_{\hexagon} - P_{\hexagon}^{-1}), \qquad (3)$$

where the sum in the second term runs over all hexagonal plaquettes, and the operators $P_{\hexagon}$ and $P_{\hexagon}^{-1}$ permute the configuration on a hexagon clockwise and anticlockwise (also called ring-exchange terms). The new term directly couples to the scalar chirality on the hexagons, breaks time-reversal invariance, and is a bona fide SU(6) generalization of an SU(2) Hamiltonian on the kagome lattice which has been shown to give rise to an extended SU(2) chiral spin liquid phase [34,35]. Alternatively it can be viewed as a drastically truncated version of a parent Hamiltonian for a SU(N) chiral spin liquid [36]. In the following, we will discuss the properties of that model as a function of θ, noting that $\theta = 0$ corresponds to the pure Heisenberg model (1).

The ED spectrum on 24 sites (Fig. 5) shows a clear change of behavior between the small θ range, with a twofold excited state well separated from the rest of the spectrum, and the range above $\theta \simeq 0.2$, where a manifold of six singlet states becomes almost degenerate and very well separated from the rest of the spectrum. Two of these states are at the Γ point, and the remaining four are at the K points, in agreement with the momenta of the six chiral VMC states (discussed below). So, the ED results are clearly consistent with a phase transition between a plaquette phase and a chiral phase upon increasing the ring-exchange term. Note that the degeneracy of the chiral state is only equal to 6 and not 12 because the Hamiltonian of Eq. (3) explicitly breaks the time-reversal symmetry.

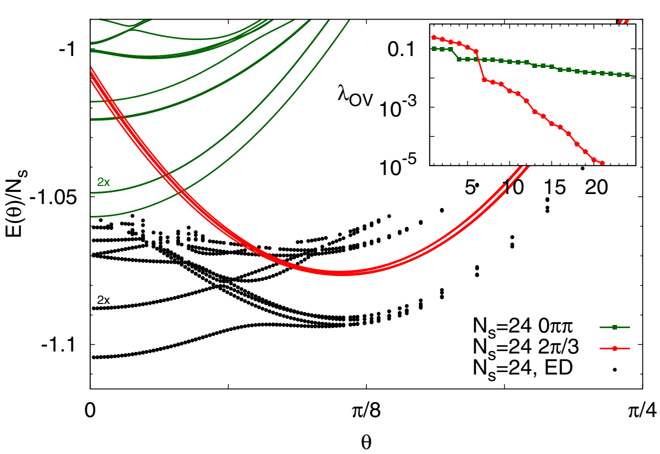

FIG. 5. Comparison of the ED spectrum (black points) of the model of Eq. (3) with the variational energies (continuous lines) based on Gutzwiller projected wave functions for the $0\pi\pi$ plaquette phase and the $2\pi/3$ chiral phase. The inset shows the (ordered) eigenvalues λ_j of the overlap matrices of the projected states with different twisted boundary conditions before projection as a function of j.

This interpretation is further supported by the comparison with VMC on 24 sites. To access the low energy spectrum and not just the ground state, we have constructed a large family of Gutzwiller projected states by changing the boundary conditions (BCs) of the fermionic wave functions [37], considering up to 30 different BCs for the $2\pi/3$ flux states, and up to 90 for the $0\pi\pi$ flux states (30 for each translation breaking state), and we have diagonalized the overlap matrix and the Hamiltonian in this variational subspace [38,39]. The results are summarized in Fig. 5. For the chiral state, this parton construction leads to six (and only six) significant eigenvalues of the overlap matrix, which themselves lead to six low-lying states very close in energy [40]. There is not such a clear cutoff for the plaquette states, and the three low-lying states are not so well split from the other states. Although the variational plaquette and chiral states are higher in energy, their overall behavior is qualitatively consistent with ED. In particular, the energy of the plaquette state is minimal at $\theta = 0$, while that of the chiral states is minimal around $\theta = 0.36$, and their energies cross around $\theta = 0.16$.

Similar overlap calculations were carried out for $N_s = 72$ sites, with 30 different BCs for the $2\pi/3$ flux case, and 12 for each translation breaking state (36 in total) for the $0\pi\pi$ flux case. The energy corrections for the $0\pi\pi$ case turn out to be larger (see Table I), again promoting the plaquette-ordered phase over the chiral liquid phase at the Heisenberg point [41].

Interestingly, Gutzwiller projected wave functions turn out to be much better for the chiral phase than for the plaquette phase on 24 sites. In fact, the energy minimum for the $0\pi\pi$ flux states, shown in Fig. 1, occurs for $t_d/t_h \approx -0.85$. Now, for $t_d \leqslant -t_h/2$, which includes the optimal energy value, the fermionic wave function is gapless at the Fermi energy: the lowest band (the only filled one) touches the empty band above it at the Γ point (the Fermi surface is confined to a point) [14]. So, by contrast to the plaquette phase of the SU(3) Heisenberg on the honeycomb lattice, which is described by a gapped fermionic wave function [14], the plaquette phase discussed here for SU(6) corresponds to a gapless spectrum before projection, hence possibly also to a gapless spectrum after projection. Since this gapless point is not protected (the spectrum is gapped for $t_d > -t_h/2$), we suspect that this is an artifact, and that adding additional terms in the fermionic Hamiltonian might open a gap and further lower the variational energy of that state. This is supported by the fact that the variational energy of the plaquette phase obtained with VMC is much higher than that obtained by iPEPS for the same phase.

Discussion. Altogether, we believe that the numerical results reported in this Rapid Communication provide compelling evidence in favor of a plaquette ground state for the SU(6) Heisenberg model on the honeycomb lattice. We have also shown that there is, however, a chiral phase close by in parameter space. In particular, let us emphasize that the variational energy obtained by iPEPS for the plaquette state is much lower than that of the chiral state obtained by VMC, which, as shown when introducing a ring-exchange term, is very good at describing the chiral phase. This situation is reminiscent of the SU(2) honeycomb model for intermediate values of the next-nearest-neighbor exchange interaction ($J_2/J_1 \approx 0.3$): Several numerical methods [42–46] found a plaquette-ordered phase, while mean-field [47], variational Monte Carlo [48], and entangled-plaquette variational ansatz [49] approaches could not reproduce these results but reported instead gapped spin liquid/columnar valence bond solid phases in that parameter range.

Even if it led to the wrong conclusion, the mean-field approach should be given credit for identifying the right candidates with very similar energies [17]. This lends further support to the mean-field prediction by Hermele *et al.* [15,16] of a chiral phase for several particles per site since there does not seem to be competing VBS states too close in energy in that case. Numerical work along the lines of the present Rapid Communication to test this prediction is in progress.

Acknowledgments. This work has been supported by the Swiss National Science Foundation, the JSPS KAKENHI Grant No. 2503802, by the Hungarian OTKA Grant No. K106047, by the National Science Foundation under Grant No. NSF PHY11-25915, by the Austrian Science Fund FWF (F-4018-N23 and I-1310-N27), and by the Delta-ITP consortium [a program of the Netherlands Organisation for Scientific Research (NWO) that is funded by the Dutch Ministry of Education, Culture and Science (OCW)].

[1] C. Wu, J.-p. Hu, and S.-c. Zhang, Phys. Rev. Lett. **91**, 186402 (2003).
[2] C. Honerkamp and W. Hofstetter, Phys. Rev. Lett. **92**, 170403 (2004).
[3] M. A. Cazalilla, A. F. Ho, and M. Ueda, New J. Phys. **11**, 103033 (2009).
[4] A. V. Gorshkov, M. Hermele, V. Gurarie, C. Xu, P. S. Julienne, J. Ye, P. Zoller, E. Demler, M. D. Lukin, and A. M. Rey, Nat. Phys. **6**, 289 (2010).
[5] S. Bieri, M. Serbyn, T. Senthil, and P. A. Lee, Phys. Rev. B **86**, 224409 (2012).
[6] F. Scazza, C. Hofrichter, M. Höfer, P. C. De Groot, I. Bloch, and S. Fölling, Nat. Phys. **10**, 779 (2014).
[7] S. Taie, R. Yamazaki, S. Sugawa, and Y. Takahashi, Nat. Phys. **8**, 825 (2012).
[8] G. Pagano, M. Mancini, G. Cappellini, P. Lombardi, F. Schäfer, H. Hu, X.-J. Liu, J. Catani, C. Sias, M. Inguscio, and L. Fallani, Nat. Phys. **10**, 198 (2014).
[9] X. Zhang, M. Bishof, S. L. Bromley, C. V. Kraus, M. S. Safronova, P. Zoller, A. M. Rey, and J. Ye, Science **345**, 1467 (2014).
[10] M. A. Cazalilla and A. M. Rey, Rep. Prog. Phys. **77**, 124401 (2014).
[11] T. A. Tóth, A. M. Läuchli, F. Mila, and K. Penc, Phys. Rev. Lett. **105**, 265301 (2010).
[12] P. Corboz, M. Lajkó, A. M. Läuchli, K. Penc, and F. Mila, Phys. Rev. X **2**, 041013 (2012).
[13] P. Corboz, K. Penc, F. Mila, and A. M. Läuchli, Phys. Rev. B **86**, 041106 (2012).
[14] P. Corboz, M. Lajkó, K. Penc, F. Mila, and A. M. Läuchli, Phys. Rev. B **87**, 195113 (2013).
[15] M. Hermele, V. Gurarie, and A. M. Rey, Phys. Rev. Lett. **103**, 135301 (2009).
[16] M. Hermele and V. Gurarie, Phys. Rev. B **84**, 174441 (2011).
[17] G. Szirmai, E. Szirmai, A. Zamora, and M. Lewenstein, Phys. Rev. A **84**, 011611 (2011).
[18] P. Sinkovicz, A. Zamora, E. Szirmai, M. Lewenstein, and G. Szirmai, Phys. Rev. A **88**, 043619 (2013).
[19] H. Yokoyama and H. Shiba, J. Phys. Soc. Jpn. **56**, 1490 (1987).
[20] C. Gros, Ann. Phys. **189**, 53 (1989).
[21] X. G. Wen, F. Wilczek, and A. Zee, Phys. Rev. B **39**, 11413 (1989).
[22] P. Nataf and F. Mila, Phys. Rev. Lett. **113**, 127204 (2014).
[23] F. Verstraete and J. I. Cirac, arXiv:cond-mat/0407066.
[24] T. Nishino, Y. Hieida, K. Okunishi, N. Maeshima, Y. Akutsu, and A. Gendiar, Prog. Theor. Phys. **105**, 409 (2001).
[25] J. Jordan, R. Orús, G. Vidal, F. Verstraete, and J. I. Cirac, Phys. Rev. Lett. **101**, 250602 (2008).
[26] P. Corboz, S. R. White, G. Vidal, and M. Troyer, Phys. Rev. B **84**, 041108 (2011).
[27] P. Corboz, T. M. Rice, and M. Troyer, Phys. Rev. Lett. **113**, 046402 (2014).
[28] T. Nishino and K. Okunishi, J. Phys. Soc. Jpn. **65**, 891 (1996).
[29] R. Orús and G. Vidal, Phys. Rev. B **80**, 094403 (2009).
[30] P. Corboz, R. Orus, B. Bauer, and G. Vidal, Phys. Rev. B **81**, 165104 (2010).
[31] H. N. Phien, J. A. Bengua, H. D. Tuan, P. Corboz, and R. Orus, Phys. Rev. B **92**, 035142 (2015).
[32] S. Singh, R. N. C. Pfeifer, and G. Vidal, Phys. Rev. B **83**, 115125 (2011).
[33] B. Bauer, P. Corboz, R. Orús, and M. Troyer, Phys. Rev. B **83**, 125106 (2011).
[34] B. Bauer, L. Cincio, B. P. Keller, M. Dolfi, G. Vidal, S. Trebst, and A. W. W. Ludwig, Nat. Commun. **5**, 5137 (2014).
[35] A. Wietek, A. Sterdyniak, and A. M. Läuchli, Phys. Rev. B **92**, 125122 (2015).
[36] H.-H. Tu, A. E. Nielsen, and G. Sierra, Nucl. Phys. B **886**, 328 (2014).
[37] Y. Zhang, T. Grover, A. Turner, M. Oshikawa, and A. Vishwanath, Phys. Rev. B **85**, 235151 (2012).
[38] T. Li and F. Yang, Phys. Rev. B **81**, 214509 (2010).
[39] J.-W. Mei and X.-G. Wen, arXiv:1407.0869.
[40] P. Nataf, M. Lajkó, A. Wietek, K. Penc, F. Mila, and A. M. Läuchli, arXiv:1601.00958.
[41] Note that while the diagonal energies depend on the value of t_d/t_h, the spanned subspace of the projected states with different boundary conditions before projection remains the same, thus the optimized energies are independent of small changes of t_d/t_h.
[42] H. Mosadeq, F. Shahbazi, and S. A. Jafari, J. Phys.: Condens. Matter **23**, 226006 (2011).

[43] A. F. Albuquerque, D. Schwandt, B. Hetényi, S. Capponi, M. Mambrini, and A. M. Läuchli, Phys. Rev. B **84**, 024406 (2011).

[44] S.-S. Gong, W. Zhu, and D. N. Sheng, Phys. Rev. B **92**, 195110 (2015).

[45] R. Ganesh, J. van den Brink, and S. Nishimoto, Phys. Rev. Lett. **110**, 127203 (2013).

[46] R. F. Bishop, P. H. Y. Li, and C. E. Campbell, J. Phys.: Condens. Matter **25**, 306002 (2013).

[47] H. Zhang and C. A. Lamas, Phys. Rev. B **87**, 024415 (2013).

[48] B. K. Clark, D. A. Abanin, and S. L. Sondhi, Phys. Rev. Lett. **107**, 087204 (2011).

[49] F. Mezzacapo and M. Boninsegni, Phys. Rev. B **85**, 060402 (2012).